Revista de metalurgia

Evaluation of cold crack susceptibility on HSLA steel welded joints(•)

R.C. Silverio-Freire Júnior*, T. Moura-Maciel** y P. Guedes da Silva**

Abstract

The present study addresses an evaluation of the effect of several welding parameters on cold cracking formation in welded joints of High Strength and Low Alloy steels, as well as the resulting microstructures and hardness values. The main parameters studied include the variation of the preheating temperature, drying time of the electrode, chemical composition and thickness of the base metal. The presence of cold cracking in the joints was analyzed from Tekken tests using steel plates made of SAR 80 T, 100 T and 120 T with of various thickness. The plates were welded by Shielded Metal Arc Welding either with or without pre-heating. Different preheating temperatures were studied, i.e., 375, 455 and 525 K. AWS E 12018 G and 11018 G electrodes were used under different conditions, i.e., not dried or dried up to 2, 3 and 4 h at 515 K. The results indicated the presence of cracks in the welded metals with the combination of hardness values above 230 HV and the formation of high contents of acicular ferrite (above 93 %) in the welds without preheating. Higher crack susceptibility was also observed in the thick welded metal plates.

Keywords Cold cracking. HSLA steels. Microstructure. Tekken tests.

Evaluación de la susceptibilidad de formación de fisuras en frío en juntas soldadas de aceros de alta resistencia y baja aleación

Resumen

Este trabajo evalúa la influencia de la variación de temperatura de precalentamiento, del tiempo de secado del electrodo, de la composición química y del espesor del metal base sobre la formación de fisuras en frío, inducidas por el hidrógeno en juntas soldadas de aceros de alta resistencia y baja aleación y su relación con la microestructura y dureza resultante. Para esto, se analizó la presencia de fisuras en frío en probetas para ensayos Tekken, fabricadas a partir de chapas de aceros SAR 80 T, 100 T y 120 T, con diferentes espesores y soldados por proceso de arco eléctrico con electrodo revestido, sin precalentamiento y con precalentamiento, a 375, 455 y 525 K, empleando electrodos AWS E 12018 G y 11018 G no secados y secados durante 2, 3 y 4 h. Los resultados obtenidos indicaron la presencia de fisuras únicamente en la zona de metal de aporte con una combinación de los valores de dureza superiores a 230 Hv y con porcentajes de ferrita acicular superiores al 93 %, obtenidos sin precalentamiento. Además de ello, en las chapas de mayor espesor, se obtuvo una mayor susceptibilidad a la fisuración en frío, aunque presentasen menor valor de carbono equivalente.

Palabras clave Fisuras en frío. Aceros de alta resistencia y baja aleación. Microestructura. Ensayos Tekken.

1. INTRODUCTION

Relevant technological progress has taken place during the last decades towards the development of new materials. In particular, steels stand out as the globally most used among marketed materials. Consequently, new types of steels with relatively high tensile strength and improved toughness have been developed. For example, high-strength and low-alloy steels (HSLA). Nevertheless, one of the main requirements for the commercialization of a new type of steel is its weldability. Therefore, new technologies have been developed in this area aiming at expanding the range of applications for new steels.

(•) Trabajo recibido el día 5 de abril de 2002 y aceptado en su forma final el día 24 de marzo de 2003.

(*) Federal University of Rio Grande do Norte. Center of Exact Sciences and Earth. Program of Doctorate in Science and Enginnering of Materials. CEP 59072970, Natal, RN, Brasil. E-mail: freirej@ufrnet.br

(**) Federal University of Paraiba. Center of Science and Technology, Dept. of Mechanical Engineering. Campus II. CEP 58. 109-970, Campina Grande, PB, Brasil. E-mail: theo@dem.ufpb.br

Hydrogen-induced cold cracking is one of the main problems encountered for welding of high-strength and low-alloy steels (HSLA). For this reason, at least 20 % of the large sum (billions of dollars) spent by industries worldwide are committed to solve this problem.

The main aspects which contribute to cold cracking are the high contents of diffusive hydrogen, temperature in the welded joint below 475 K, brittleness and the high levels of residual stresses remaining at the welded joint[1 and 2]. All these elements are significantly affected by the variation of cooling time ($\Delta T_{8/5}$) at the weld joints, which, in turn, can be adjusted by changing heat input, preheating temperature or thickness of the plate. In addition, electrode drying and cooling time play an important role on determining diffusive hydrogen in welded joints. The effect of the aforementioned issues is intensified in welded joints with elevated hardness. For this reason, hardness tests are widely used to evaluate the susceptibility of the joints to this type of defect [3].

Usually, hydrogen-induced cold cracking begins and propagates in the heat-affected zone, due to its microstructure, which results in high hardness and brittleness[4 and 5]. It can also take place in the welded metal if it develops high hardness and the restriction to dilatation is very high[6].

Cold cracking in HSLA steels welded joints was evaluated in this work. The following parameters were investigated: preheating temperature, electrode drying, combination between base metal and deposited metal, and variation of the thickness of the base metal.

2. MATERIALS AND METHODS

Shield Metal Arc Welding (SMAW) was employed using AWS E 12018 G and AWS E 11018 G consumable electrodes. The base metal plates consisted of commercially available SAR 120 T (ASTM A 514 B), SAR 100 T (ASTM A 514 F) and SAR 80 T steel plates 31 mm, 11 mm and 11 mm thick, respectively.

The presence of cracks was evaluated using the Tekken test (JIS-Z-3158 standard). This test consists in welding specimens with the dimensions indicated in figure 1 and observing the presence of cracks 48 h later. To that end specimens are cut into eight similar (or identical) parts.

The heat input was calculated from the voltage of the welding equipment and the welding time using equation (1). The current was indirectly estimated

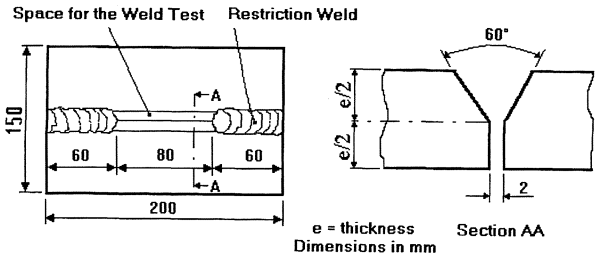

Figure 1. Schematics of the specimen for the Tekken test.

Figura 1. Esquema de las probetas para ensayos Tekken.

starting from a "shunt" of 200 A / 60 mV in series with the machine. The following relation was used:

$$E = f \times \frac{VI}{v} \times 10^{-3} \qquad (1)$$

The values of E, V, I and v represent, respectively, the heat input (kJ/mm), the voltage (Volts), current (A) and welding speed (mm/s). The value of f is 0.8 and represents the arc heat transfer efficiency of Shield Metal Arc Welding.

Welding was carried out using around 2 kJ/mm of heat input. The base metal was either pre-heated or not. Pre-heating temperatures were set to 375, 455 and 525 K. The electrodes were used either without drying or dried up during 2, 3 or 4 h at 515 K for three combinations of steel/electrode, i.e., SAR 120T steel and AWS E 12018 G electrode, SAR 100 T steel and AWS E 12018 G electrode, and SAR 80 T steel and AWS E 12018 G electrode. The combination SAR 100 T steel with AWS E 11018 G electrode was tested only with electrodes that were not dried due to the absence of cracking in all specimens. This includes those which were not pre-heated. Three tests were carried out for each condition, totaling 156 tests. The results obtained for each condition were identical for all three specimens tested.

The following expression was used for the calculation of the Carbon Equivalent (CE), according to guidelines of the International Institute of Welding (IIW) [7].

$$CE = C + \frac{Mn}{6} + \frac{Cr + Mo + V}{5} + \frac{Ni + Cu}{15} \qquad (2)$$

To simplify the nomenclature throughout the paper, codes for each combination of base metal and filler metal were employed. For instance, the combination of SAR 120T steel with AWS E 12018 G electrode was labeled 120T/E12018.

Likewise, SAR 100 T and AWS E 12018 G was labeled 100T/E12018, SAR 80 T and AWS E 12018 G, 80T/E12018 and finally, SAR 100 T and AWS E 11018 G, 100T/E11018.

The chemical compositions and tensile strengths of steels and electrodes are shown in table I. For the chemical analyses of the weld metal each combination of base metal and filler metal was sent to USIMINAS (see Table II). Both X-ray fluorescence spectrometry and plasma spectrometry were carried out.

Point identification and counting were performed using micrographs at 400 times magnification. A screen with 100 points was drawn and positioned on the display of the microscope. The intersections of the lines of the screens assisted in analyzing the microstructure. After the identification of all areas, the points were counted. Fourteen areas were analyzed in each weld metal, and since the bars contained 100 points, 1400 points were totalized per sample. It is important to point out that microstructural analyses were not carried out for welded specimens preheated at 455 K or dried specimens.

To evaluate the effect of the hardness of the weld metal on cold crack formation, the specimens were submitted to Vickers hardness tests using a load of 5 kg. Indentations were made on the upper, lower and central areas of the weld metal. For each region, 5 measurements were made, totaling 15 measurements per sample. It is important to point out that all the specimens were submitted to hardness tests.

3. RESULTS AND DISCUSSIONS

No cracks were observed on the heat-affected zone of any sample. In most of the cases, the cracks began at the root and propagated until the surface of the weld metal. However, two cracks were sometimes observed, as is illustrated in figure 2. No cracks were observed in weld metals obtained from the 100T/E11018 combination.

Figures 3 and 4 illustrate the influence of the relationship between preheating temperature and electrode drying time on cold cracking of weld metals obtained from the 120T/E12018 and 100T/E12018 combinations, respectively. For 80T/E12018, cracks were only obtained on the specimens without preheating. It could then be established that welded joints free of cold cracking were only obtained using one or two of these parameters.

The minimum conditions established during the tests to prevent cracks in the welded joints are listed in table III. The AWS E 12018 G electrode revealed little weldability if compared with AWS E 11018 G, because whereas AWS E 12018 G requires extensive caution in its application, regardless of the base metal used, the weld metal obtained with the SAR 100T plate welded with AWS E 11018 G did not show any cracks,

Table I. Chemical composition and tensile strength of SAR 80T, SAR 100 T and SAR 120 T steels and AWS E 11018 G and AWS E 12018 G electrodes

Tabla I. Composición química y resistencia a tracción de los aceros SAR 80T, SAR 100 T y SAR 120 T y de los electrodos AWS E 11018 G y AWS E 12018 G

Element	Steel SAR 80 T	Steel SAR 100 T	Steel SAR 120 T	Electrode AWS E 11018 G	Electrode AWS E 12018 G
C	0.11	0.16	0.16	0.06	0.079
S	0.09	0.04	0.07	0.024	0.0065
Mn	0.98	0.93	0.84	1.6	1.76
Si	0.25	0.26	1.12	0.3	0.28
P	0.21	0.16	0.14	0.018	0.018
Cr	0.61	0.67	0.96	0.35	0.50
Cu	0.24	0.32	0.01	0.011	0.028
Mo	0.48	0.45	0.15	0.4	0.34
V	0.42	0.53	0.06	0.02	0.010
Ni	0.03	1.11	1.27	1.7	1.82
Nb	–	0.002	0.002	–	< 0.002
B	0.15	0.0007	0.12	< 0.0002	0.0007
Tensile Strength	887 MPa	1005 MPa	1332 MPa	780 MPa	1053 MPa

Table II. Chemical composition and carbon equivalent of weld metals

Tabla II. Valores de la composición química y carbono equivalente en la zona del metal de aportación

Element	100T/E12018	120T/E12018	80T/E12018	100T/E11018
C	0.099	0.094	0.087	0.083
Mn	1.552	1.585	1.557	1.446
Cr	0.542	0.587	0.529	0.424
Cu	0.101	0.025	0.083	0.082
Mo	0.368	0.304	0.376	0.412
V	0.140	0.020	0.117	0.137
Ni	1.642	1.716	1.355	1.564
CE	0.684	0.657	0.647	0.628

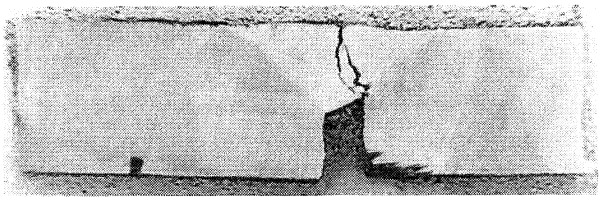

Figure 2. Position and size of cracks in the Tekken specimen.

Figura 2. Posición y tamaño de las fisuras en las probetas Tekken.

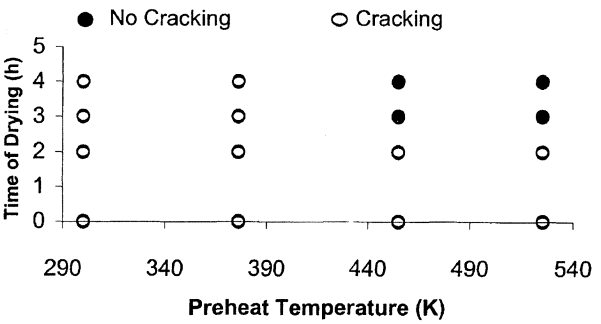

Figure 3. Influence of preheating temperature and electrode drying time on cold cracking of the combination of base metal and 120T/E12018 electrode.

Figura 3. Influencia de la variación de la temperatura de precalentamiento y del tiempo de secado del electrodo sobre la formación de fisuras en frío, para la combinación de metal base y electrodo 120T/E12018.

including welds without preheating and electrodes not dried.

The main microconstituents observed in the weld metals were primary ferrite, secondary ferrite and acicular ferrite[8]. The presence of this last phase is considered desirable in weld metals to improve toughness and hinder crack propagation, due to its small grains and high contour angles[1, 9 and 10].

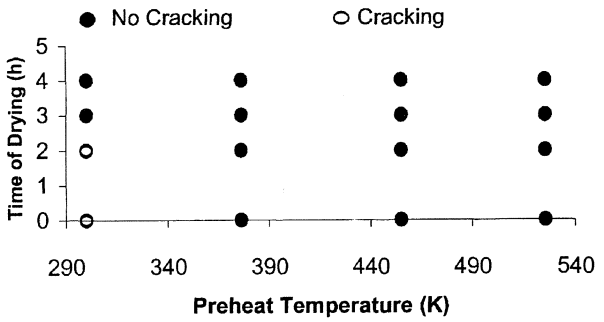

Figure 4. Influence of preheating temperature and electrode drying time on cold cracking of the combination of base metal and 100T/E12018 electrode.

Figura 4. Influencia de la variación de la temperatura de precalentamiento y del tiempo de secado del electrodo sobre la formación de fisuras en frío, para la combinación de metal base y electrodo 100T/E12018.

However, contents of acicular ferrite in excess of 87 % can excessively harden the ferritic matrix, harming the weld metals toughness and assisting cold cracking formation[11]. The effect of hardness and acicular ferrite contents on cold crack formation in welded joints obtained without drying the electrode can be analyzed from figure 5. The susceptibility to cracking on the weld drastically increased as hardness and acicular ferrite contents increase to 300 HV and 93 %, respectively. On the other hand, the individual action of just one parameter, especially hardness, does not necessarily results in cold cracking. This result is somehow in good agreement with other studies[6 and 12] which reported that susceptibility to cold cracking of the weld metal increased above 300 HV. Furthermore, it has also been suggested[3] that for high contents of hydrogen, hardness rules the susceptibility to cold cracking. Such high hardness values of the weld metals and the auto-restriction of the test can justify cracking only in this region of the welded joint. It can also be observed from figure 5 that most of the conditions that resulted in cracking took place in the weld metals obtained without preheating, demonstrating the importance of such treatment to prevent cracking of welded joints [8, 13 and 14].

Considering the effect of the thickness of the sample on cold crack formation, welds with electrodes AWS E12018 using SAR 120 T 31 mm or SAR 100 T 11 mm, were compared. The relationship between thickness and the smallest value of hardness that resulted in cold cracking (critical hardness) is shown in figure 6. The results indicated that the critical hardness for the thicker plate was 327 HV, whereas for the thinner plate, it

Table III. Minimum conditions necessary to prevent cracking of the welded joint

Tabla III. Condiciones mínimas mantenidas durante los ensayos en que no se observó ninguna fisura en la juntura soldada

Combination base metal - electrode	Weldability	Minimum condition for joint without cracking
SAR 120 T steel with AWS E 12018 G electrode	Bad	Pre-heating temperature of at least 455 K and drying the electrode for at least 3 h at 515 K
SAR 100 T steel with AWS E 12018 G electrode	Reasonable	Pre-heating temperature of at least 375 K or drying the electrode for at least 3 h at 515 K
SAR 80 T steel with AWS E 12018 G electrode	Reasonable	Pre-heating temperature of at least 375 K
SAR 100 T steel with AWS E 11018 G electrode	Good	No Pre-heating and electrode not dried

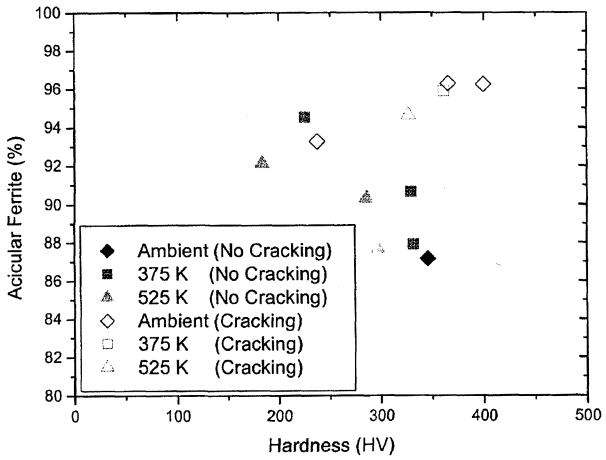

Figure 5. Analysis of the effect of the contents of acicular ferrite and hardness on cold cracking using electrodes without drying.

Figura 5. Relación entre el porcentaje de ferrita acicular y la dureza en la zona del metal de aportación, donde se presentaron fisuras utilizando electrodos no secados.

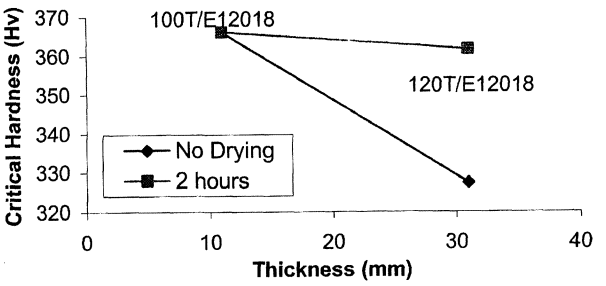

Figure 6. Relationship between thickness and critical hardness for cold cracking in weld metal.

Figura 6. Relación entre la espesor y dureza crítica para la formación de las fisuras en frío en la zona del metal de aportación.

was 366 HV, for welding using electrodes without drying. It is important to point out that CE is larger in the 100E12018 combination compared to 120E12018 (Table II), implying that the 100E12018 combination has a higher probability for cold cracking and, consequently, lower critical hardness compared to 120E12018. However, that was not verified, only the increase in the thickness of SAR 120 T steel can explain the fact that the 120E12018 combination has a smaller critical hardness than 100E12018.

From figure 6 it could also be seen that the shorter cooling time of thick plates provide shorter time to drive hydrogen out of the joint thus increasing the risk of cracking due to the formation of a brittle microstructure[15]. Using electrodes dried for 2 h, the critical hardness of the thicker sample increased, revealing the need for drying the electrode to obtain a welded joint free of cold cracks. The critical hardness for drying times of 3 and 4 h was not determined since no cold cracks were observed on the 100T/E12018 combination (as shown in figure 4) for such drying times. Therefore, the results could not be compared in that case.

It is important to note that in the analysis of cold cracking formation, both the carbon equivalent values and the microstructure of the weld metal influence cold crack susceptibility of the welded joint. As the microstructure is related to the chemical composition of the weld metal, the examination of the influence of the carbon equivalent in the microstructure of the weld metal is very important to obtain a detailed analysis of all the parameters that can affect cold cracking formation. The influence of the carbon equivalent

on the microstructure of weld metal specimens welded without preheating is shown in figure 7. In addition, in figure 7 and figure 8, the first curve shows the values of AF, the second one is the sum of AF and FS. The sum of AF, FS and PF should account for all of the microstructure (100 %). The results obtained for the 120E12018 combination, were not used because of its different thickness compared to the others. This parameter significantly affects the microstructure since it changes the cooling time ($\Delta t_{8/5}$), and consequently, the formation of microconstituents[1-3]. From figure 7, it can be noticed that the contents of acicular ferrite increased 9.12 % by increasing the Carbon Equivalent in 0.056 [16 and 17]. In addition, the carbon equivalent had a significant effect on the decrease of the contents of primary ferrite (PF) and secondary ferrite (FS). The former decreased from 6.25 % to 2.31 % and the latter from 6.6 % to 1.4 %.

As observed previously, the increase in the carbon equivalent contributed significantly to the increase in the contents of acicular ferrite in specimens welded without preheating. However, such effect was suppressed by preheating the sample at 525 K, as shown in figure 8. This demonstrated the significant contribution of high preheating temperatures on the cooling rate and, consequently, on the formation of the microstructure of the weld metal. Moreover, the contents of primary ferrite were little affected by the increase in the carbon equivalent, increasing from 5.9 % to 7 %.

Figures 9 and 10 show the variation of the contents of acicular ferrite and primary ferrite with increasing preheating temperature for different

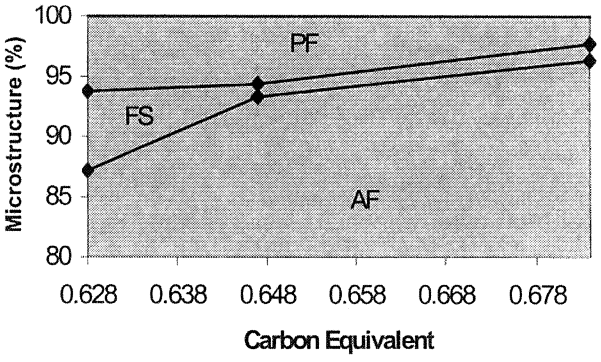

Figure 7. Effect of carbon equivalent on the microstructure of weld metals welded without preheating.

Figura 7. Influencia del carbono equivalente sobre la microestructura de la zona del metal de aportación en las probetas soldadas sin precalentamiento.

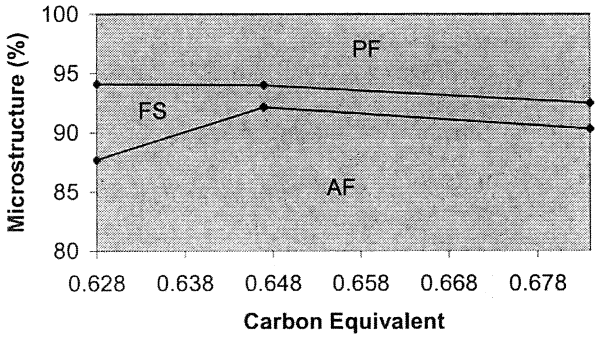

Figure 8. Effect of carbon equivalent on the microstructure of he weld metals welded after preheating at 525 K.

Figura 8. Influencia del carbono equivalente sobre la microestructura de la zona del metal de aportación en las probetas soldadas con precalentamiento de 525 K.

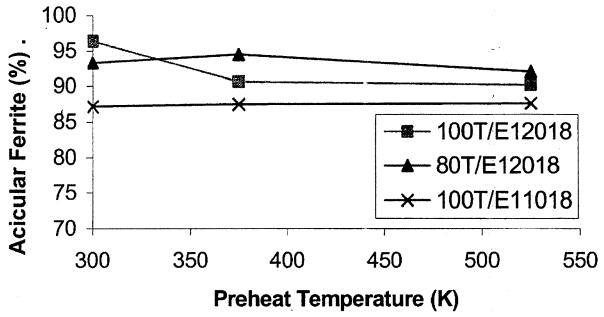

Figure 9. Effect of preheating temperature on the percentage of acicular ferrite for various combinations of base metal and electrode.

Figura 9. Influencia de la temperatura de precalentamiento en el porcentaje de ferrita acicular para varias combinaciones de metal base y electrodo.

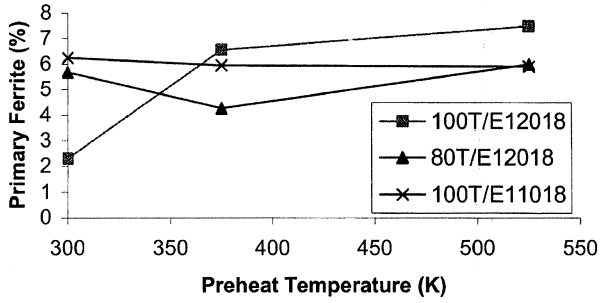

Figure 10. Effect of preheating temperature on the percentage of primary ferrite for various combinations of base metal and electrode.

Figura 10. Influencia de la temperatura de precalentamiento en el porcentaje de ferrita primaria para varias combinaciones de metal base y electrodo.

combinations of base metal and deposited metal. Once more, the results obtained for 120E12018 were not used since such combination was thicker

than all the others. The contents of acicular ferrite obtained herein exceeded those reported by Vercesi[18], who obtained percentages between 62 % and 74 % welding AWS A5.5-81 19 mm with AWS E 11018-M and AWS E 12018-M electrodes using heat input around 1.7 kJ/mm. From these figures it could be seen that the 100T/E11018 combination did not reveal significant variation in the percentage of acicular and primary ferrite.

Finally, for the 100T/E12018 combination, there was a discrete decrease in the percentage of acicular ferrite and, consequently, an increase in the percentage of primary ferrite. In addition, the contents of acicular ferrite for the combinations in which the AWS E 12018 G electrode was used were higher than those for combinations involving AWS E 11018 G, as shown in figure 9. As this value was around 93 %, it provided excessive hardening in the weld metal, which certainly contributed to crack formation[11].

4. CONCLUSIONS

- Cracks were not observed in the HAZ. All cracks in the weld metals occurred using the AWS E 12018 electrode as filler metal.
- The conditions to prevent cracking in all base and filler metal combinations tested included preheating above 370 K and electrode drying for longer than two hours. Those results demonstrated the importance of these welding parameters to obtain joints free from cold cracking.
- The formation of acicular ferrite contents above 93 % combined with hardness values above 300 HV in the weld metal of HSLA steels increased the susceptibility for cold cracking.
- The use of the AWS E12018 G electrode is only possible after its drying or preheating the base metal.
- The variation of the equivalent carbon had an important effect on determining the microstructure of weld HSLA steel. Increasing the carbon equivalent increased the contents of acicular ferrite in the welded joint.
- The effect of preheating temperature on the microstructure depended on the specific weld joint/base metal combination, either decreasing or maintaining the content of acicular ferrite.

ACKNOWLEDGMENTS

The authors thank ESAB for the donation of the consumables, USIMINAS (group SIDERBRAS) for the donation of the plates, CNPQ/PIBIC/UFPB and CAPES for the scholarship grant.

DEDICATORY

We dedicate this work to the memory of Paulo Guedes da Silva, former master's student of our institution. God be to his side.

REFERENCES

[1] E. WAINER, S.D. BRANDI and F.D.H. MELLO, *Soldagem Processos e Metalurgia*, Ed. Edgard Blücher LTDA, 1° Ed., São Paulo-SP-Brasil, 1992, pp. 419-425.

[2] V.I. SHVACHKO, *Int. J. Hydrogen Energy* 25 (2000) 473-480.

[3] P.H.M. HART, *Weld. J.* 9-10 (1986) 190-198.

[4] X. DI-JING, Q. HONG and J. JIANMING, *Weld. J.* 12 (1994) 164s-171s.

[5] B.S. KASATKIN and S.B. KASATKIN, *Weld. J.* 7 (1998) 299s-306s.

[6] N.G. ALCANTARA and J.H. ROGERSON, *Weld. J.* 4 (1984) 116-122.

[7] IIW/IIS DOC. 452-74, Welding in the World, 12(3/4), 1974, pp. 65-69.

[8] T.M. MACIEL, R.C.S. FREIRE JÚNIOR and P.G. DA SILVA, 8° *Congr. Chileno de Ingeniería Mecánica*, 1998, pp. 575-578.

[9] D. WANG, Tesis Doctoral, School of Industrial Science, Cranfield Institute of Technology, 1990.

[10] S.H. MARTINS, Dissertação de Mestrado, Prog. Pós-Grad. Ciência Eng. Materiais, Univ. Fed. São Carlos, 1990.

[11] R.A. FARRAR and P.L. HARRINSON, *J. Mater. Sci.* 22 (1987) 3812-3820.

[12] W. GARCIA, Dissertação de Mestrado, Prog. Pós-Grad. Ciência Eng. Materiais, Univ. Fed. São Carlos, 1994.

[13] T.M. MACIEL, P.G. SILVA, R.C.S. FREIRE JÚNIOR and F.V. SOUZA, *12° CBECIMAT*, 1, 1996, pp. 523-526.

[14] N.G. ALCANTARA, *Simpósio de Tecnologia de Soldagem da Região Sul*, 1, 1986, pp. 31-50.

[15] C.M.F. LOPES, R.C.S. FREIRE JÚNIOR and T.M. MACIEL, *13° CBECIMAT*, 1, 1998, pp. 334-342.

[16] T.M. MACIEL, Tesis Doctoral, Prog. Pós-Grad. Ciência Eng. Materiais, Univ. Fed. São Carlos, 1994.

[17] P.L. HARRISON and R.A. FARRAR, *Metal Const.* 2 (1987) 392-399.

[18] J. VERCESI and E. SURIAN, *Weld. J.* 4 (1998) 164s-171s.